Acta Biochim Biophys Sin (2010): 30–38 | © The Author 2009. Published by ABBS Editorial Office in association with Oxford University Press on behalf of the Institute of Biochemistry and Cell Biology, Shanghai Institutes for Biological Sciences, Chinese Academy of Sciences. DOI: 10.1093/abbs/gmp107.
Advance Access Publication 8 December 2009

Structural and functional alterations of two multidomain oxidoreductases induced by guanidine hydrochloride

Ming Jiao†, Yu-Ling Zhou[1†], Hong-Tao Li, De-Ling Zhang, Jie Chen, and Yi Liang*

State Key Laboratory of Virology, College of Life Sciences, Wuhan University, Wuhan 430072, China
†These authors contributed equally to this work
[1]Present address: College of Life Sciences, Hubei University, Wuhan 430062, China
*Correspondence address. Tel: +86-27-68754902; Fax: +86-27-68754902; E-mail: liangyi@whu.edu.cn

The unfolding and refolding of two multidomain oxidoreductases, bovine liver catalase and flavoprotein bovine milk xanthine oxidase (XO), have been analyzed by fluorescence spectroscopy, circular dichroism, and activity measurements. Two intermediates, a partially folded active dimer disassembled from the native tetramer and a partially folded inactivated monomer, are found to exist in the conformational changes of catalase induced by guanidine hydrochloride (GdnHCl). Similarly, two intermediates, an active, compacted intermediate bound by flavin adenine dinucleotide (FAD) partially and an inactive flexible intermediate with FAD completely dissociated, exist in the conformational changes of XO induced by GdnHCl. The activity regains completely and an enhancement in activity compared with the native catalase or native XO is observed by dilution of catalase or XO incubated with GdnHCl at concentrations not >0.5 or 1.8 M into the refolding buffer, but the yield of reactivation for catalase or XO is zero when the concentration of GdnHCl is >1.5 or 3.0 M. The addition of FAD provides a remarkable protection against the inactivation of XO by GdnHCl under mild denaturing conditions, and the conformational change of XO is irreversible after FAD has been removed in the presence of a strong denaturing agent. These findings provide impetus for exploring the influences of cofactors such as FAD on the structure–function relationship of xanthine oxidoreductases.

Keywords catalase; xanthine oxidase; protein folding; fluorescence spectroscopy; enzymatic activity

Received: August 12, 2009 Accepted: October 25, 2009

Introduction

Catalase (hydrogen peroxide: hydrogen peroxide-oxidoreductase) is a heme-containing, highly active, and ubiquitous enzyme that occurs in almost all aerobically respiring organisms [1,2]. This enzyme functions in two ways: catalytically, decomposing hydrogen peroxide (H_2O_2) into molecular oxygen and water without the production of free radicals, and peroxidatively, oxidizing alcohols, formate or nitrite using H_2O_2 [1–4]. Catalase is thus able to protect the cells from the toxic effects of H_2O_2 [3,4]. Bovine liver catalase is a 243-kDa homotetramer containing 84 tyrosine residues and 24 tryptophan residues, and each monomer contains a high-spin Fe(III) protoporphyrin IX [5]. The denaturant-induced unfolding of catalase has been found to be a multiphasic process with stabilization of several unique oligomeric intermediates [3], and the presence of surfactants has been observed to affect the cold denaturation of catalase [6].

Xanthine oxidoreductase enzymes can exist in two enzymatic forms: xanthine dehydrogenase (XDH) and xanthine oxidase (XO) [7]. Each subunit of both forms contains four redox centers, one molybdenum (VI) center, two iron-sulphur (2Fe-2S) clusters, and one flavin adenine dinucleotide (FAD) unit [8–10]. Xanthine oxidoreductase exists mostly as XDH in the cell but can be readily converted to the oxidase form XO by oxidation of sulfhydryl residues or by proteolysis under pathological conditions [9]. XO is an important enzyme in the purine metabolism that catalyzes xanthine to uric acid in the presence of oxygen, leading to the formation of superoxide anion radical and H_2O_2 [8–10]. Therefore, one of the products of XO-catalyzed reaction is the substrate of catalase-catalyzed reaction.

The full amino acid sequences of xanthine oxidoreductase enzymes from various sources have been deduced by sequencing of the respective cDNAs or genes [9]. They all consist of approximately 1330 amino acids and are highly homologous with, e.g. the bovine milk enzyme (1332 residues) showing 90% sequence identity to the human liver enzyme (1333 residues) [11,12]. Limited proteolysis of mammalian XO with trypsin cleaves the enzyme into three fragments of 20, 40, and 85 kDa [9,11]. Comparative

sequence alignment has indicated that the two iron sulfur centers are located in the N-terminal 20-kDa fragment, FAD in the intermediate 40-kDa fragment, and the molybdenum center in the C-terminal 85-kDa fragment [9,11,13].

Tryptophan is a very useful intrinsic probe since its emission fluorescence spectrum varied with the molecular environment of the side chain, and has been widely employed in the field of protein folding [3,14,15]. FAD not only situates in the heart of the active site of XO and XDH, but is also a naturally fluorescent group-emitting green light [16]. The intensity of FAD fluorescence considerably increases when the protein has been denatured and can serve as a criterion of enzyme nativity [17].

One of the major goals of this research is to clarify the multiple unfolding processes or distinct unfolding states (or forms) of multidomain enzymes. In this study, the unfolding and refolding of two multidomain oxidoreductases, bovine liver catalase and flavoprotein bovine milk XO, were analyzed by fluorescence spectroscopy, circular dichroism (CD), and activity measurements using guanidine hydrochloride (GdnHCl) as a denaturant. Two intermediates including a partially folded active intermediate were found to exist in the conformational changes of both catalase and XO induced by GdnHCl. Information obtained from this study will be helpful to the understanding of the structure–function relationship of these two multidomain oxidoreductases.

Materials and Methods

Materials

Bovine liver catalase (Sigma-Aldrich Co., St. Louis, USA) was used without further purification. The $A^{1\%}_{1cm}$ value of 13.5 at 405 nm [18] was used for protein concentration measurements, and the activity of catalase was measured at 405 nm by the absorbance of a stable complex of ammonium molybdate with H_2O_2 remained after the decomposition of H_2O_2 catalyzed by catalase [19]. Bovine milk XO was purified from fresh bovine milk as described by Özer *et al*. [20] and the A_{280}/A_{450} ratio was 5.7. Purified XO showed only a single protein band on the native PAGE gel (**Fig. 1**) and no partially nicked peptide was observed. The concentration of XO was determined using a molar extinction coefficient of 37,800 M^{-1} cm^{-1} at 450 nm [7,21] and the activity of the enzyme was measured spectrophotometrically by monitoring the formation of uric acid from xanthine at 295 nm in the presence of oxygen [21]. The electron transfer activity of XO from xanthine (0.03 mM) to the artificial substrate 2,6-dichlorophenolindophenol (DCPIP) was determined spectrophotometrically by monitoring the absorbance of DCPIP (0.05 mM) at 600 nm [22]. Catalase and XO were incubated in various concentrations of GdnHCl at 4°C overnight; the activities

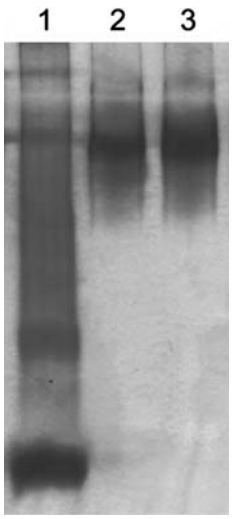

Figure 1 XO protein staining on 8% native polyacrylamide gel
Extracted filtrate was loaded on lane 1, and DEAE-Sepharose eluate was applied to lanes 2 and 3 under nonreduced conditions. Proteins in the gel were visualized by Coomassie Blue staining.

of both enzymes were determined at 25°C in the assay mixtures containing the same concentration of GdnHCl as in the original incubation. Xanthine and DCPIP were obtained from Sigma and ultra pure GdnHCl was purchased from Promega (Promega, Madison, USA). All other chemicals used were made in China and of analytical grade. The reagents were prepared in 200 mM sodium phosphate buffer (pH 7.4) for denaturation and renaturation of catalase, and 100 mM sodium phosphate buffer (pH 7.4) for XO, and these sodium phosphate buffers was also used for catalase and XO activity assays.

Intrinsic fluorescence spectroscopy

Intrinsic fluorescence spectroscopic experiments on the unfolding of catalase and XO induced by GdnHCl at different concentrations were carried out at 25°C using a LS-55 luminescence spectrometer (PerkinElmer Life Sciences, Shelton, USA). The excitation wavelength at 280 and 295 nm was used for the intrinsic fluorescence measurements of catalase and XO, respectively, and the fluorescence spectra were recorded between 300 and 400 nm. For measurement of FAD fluorescence, the excitation wavelength was 450 nm and the emission data were collected between 500 and 600 nm. The excitation and emission slits were 5 and 10 nm, respectively, and the scan speed was 100 nm/min. Assays in the absence of catalase and XO were performed to correct for GdnHCl emission fluorescence intensities.

'Phase diagram' method

The 'phase diagram' method is a sensitive approach for the detection of unfolding/refolding intermediates of proteins

[14,15,23–28]. The essence of this method is to build up the diagram of $I(\lambda_1)$ versus $I(\lambda_2)$, where $I(\lambda_1)$ and $I(\lambda_2)$ are the spectral intensity values measured on wavelengths λ_1 and λ_2 under different experimental conditions for a protein undergoing structural transformations. As spectral intensity is an extensive parameter, it will describe any two-component system by a simple Equation (1):

$$I(\lambda_1) = a + b\, I(\lambda_2) \tag{1}$$

where a and b are the intercept and slope of a plot of $I(\lambda_1)$ against $I(\lambda_2)$, respectively, and are defined by Equations (2) and (3):

$$a = I_1(\lambda_1) - \frac{I_2(\lambda_1) - I_1(\lambda_1)}{I_2(\lambda_2) - I_1(\lambda_2)} I_1(\lambda_2) \tag{2}$$

$$b = \frac{I_2(\lambda_1) - I_1(\lambda_1)}{I_2(\lambda_2) - I_1(\lambda_2)} \tag{3}$$

where $I_1(\lambda_1)$ and $I_2(\lambda_1)$ are the spectral intensities of the first and second components measured on wavelength λ_1, respectively, and $I_1(\lambda_2)$ and $I_2(\lambda_2)$ are those of the first and second components measured on wavelength λ_2, respectively. In principle, λ_1 and λ_2 are arbitrary wavelengths of the spectrum, but in practice such diagrams will be more informative if λ_1 and λ_2 will be on different slopes of the spectrum such as 320 and 365 nm for fluorescence spectra. It has been noted that application of this method to protein unfolding/refolding predicts that the dependence of I_{320} versus I_{365} will be linear if changes in the protein environment lead to all-or-none transition between two different conformations [14,15,23–26]. Here, I_{320} and I_{365} are the intrinsic fluorescence intensity values measured on wavelengths 320 and 365 nm under different experimental conditions for a protein undergoing structural transformations. On the other hand, non-linearity of this function reflects the sequential character of structural transformations. Moreover, each linear portion will describe an individual all-or-none transition. This method was employed here to detect the existence of intermediates during the unfolding of catalase and XO induced by GdnHCl. Furthermore, a mixed phase diagram based on flavin fluorescence intensity and far-UV CD data of XO was constructed to analyze the conformational transition of XO induced by GdnHCl.

Fluorescence quenching measurement

Intrinsic fluorescence quenching of XO was measured by the addition of acrylamide. The concentration of XO used in quenching experiments was 0.17 μM. Eight molar of acrylamide was prepared freshly in 100 mM sodium phosphate buffer at pH 7.4. XO (600 μl) denatured in different concentrations of GdnHCl was placed in a 0.1-cm-path length cuvette and the initial fluorescence emission intensity (F_0) was recorded. Quenching titrations with acrylamide were performed with sequentially added aliquots (2 μl) of the quencher stock solutions to the samples and gently stirred, giving a final quencher concentration ranging from 0.02 to 0.30 M. The excitation wavelength was set at 295 nm, and the corresponding emission wavelength was at 340 nm. Assays in the absence of XO were performed in order to correct for GdnHCl background fluorescence intensities. The fluorescence quenching data in the presence of acrylamide were analyzed by fitting to Stern–Volmer equation [Equation (4)] [15,29–31]:

$$\frac{F_0}{F} = 1 + K_{SV}[Q] \tag{4}$$

where F_0 and F are the fluorescence intensities in the absence and presence of quencher, $[Q]$ is the concentration of the quenchers, and K_{SV} is the Stern–Volmer quenching constant. In a protein which contains several tryptophan residues, the presence of two classes of tryptophan residues (exposed and buried) is reflected in the Stern–Volmer plot, and the K_{SV} values from Stern–Volmer equation can be used for estimating the exposed tryptophan residues in the protein [29,31].

CD measurement

CD spectra were obtained by using a Jasco J-810 spectropolarimeter (Jasco Corporation, Tokyo, Japan) with a thermostated cell holder. A quartz cell with a 1-mm light path length was used for measurements in the far-UV region. The final concentrations of XO were kept at 0.73 μM for far-UV CD. Each CD spectrum was an average of three scans and was taken from 200 to 250 nm with a scanning rate of 50 nm/min. Assays in the absence of XO were performed in order to correct for GdnHCl background CD signal. Corrected spectra were obtained by subtracting the control from sample measurements. The mean residue ellipticity $[\theta]$ (deg cm^2 $dmol^{-1}$) was calculated using Equation (5):

$$[\theta] = \frac{\theta_{obs}}{10} \frac{MRW}{lc} \tag{5}$$

where θ_{obs} is the observed ellipticity in degrees, MRW the mean residue molecular weight (108.9 Da for XO), l the path length in cm, and c the protein concentration in g/ml. Measurements were made at 25°C.

Results

Effects of GdnHCl on the activities of catalase and XO

Enzymatic activity can be regarded as the most sensitive probe for studying protein folding and unfolding, because it reflects subtle readjustments at the active site, allowing

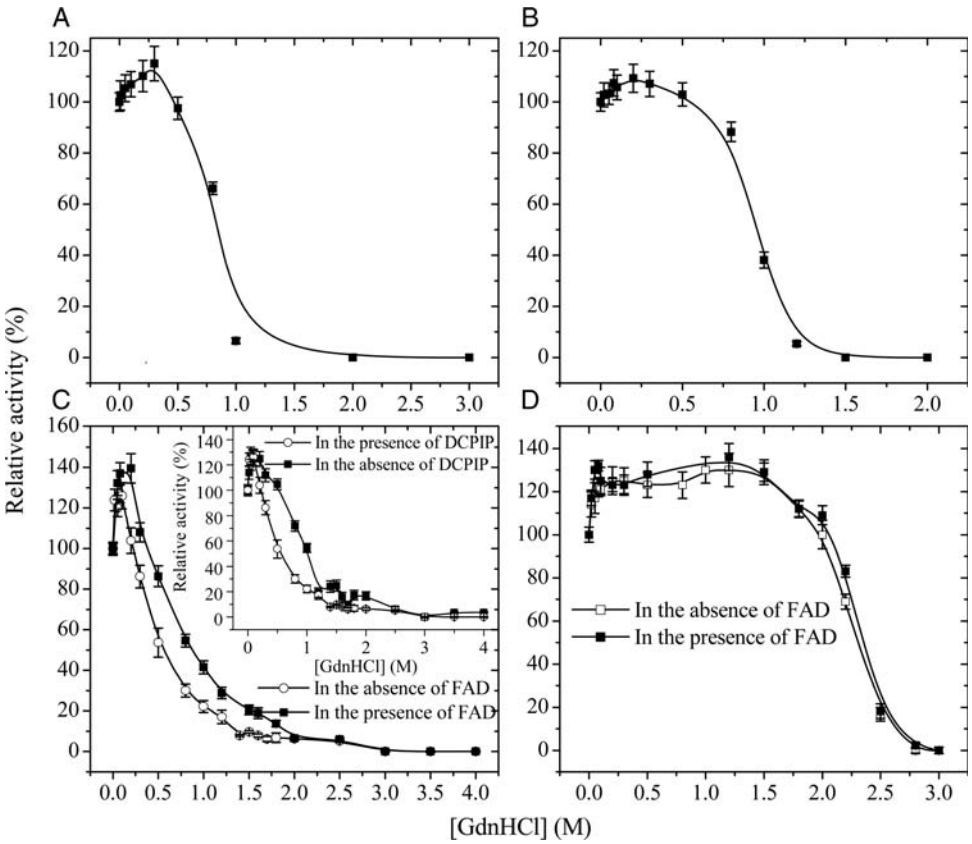

Figure 2 Activity changes of catalase and XO at different concentrations of GdnHCl The remaining activity (A) and refolding yield (B) of bovine liver catalase, and the remaining activity (C) and refolding yield (D) of bovine milk XO in the absence (open circle) and in the presence of FAD (solid square) at different concentrations of GdnHCl. The inset shows the remaining activity of XO in the absence (open circle) and in the presence of DCPIP (solid square). The concentrations of catalase were 7.6 μM (A) and 5.4 μM (B), respectively. The concentrations of XO were 0.015–0.030 μM. The refolding was monitored by recovery of enzymatic activity as a percentage of native enzyme activity. Measurements were carried out at 25°C. The data with the error bars were expressed as mean ± SD ($n = 3$).

very small conformational variations of an enzyme structure to be detected [3]. **Figure 2(A,C)** show the alterations in enzymatic activity of catalase and XO, respectively, as a function of GdnHCl concentration during unfolding. Below 0.5 M GdnHCl catalase showed peculiar behaviors. Namely, at 0.3 M GdnHCl the activity of catalase increased to about 15% above the native level, and then gradually decreased below the native level as the concentration of GdnHCl was increased to 0.8 M. A complete loss of enzymatic activity was observed when the concentration of GdnHCl reaches 1.5 M [**Fig. 2(A)**]. Similarly, an enhancement in the XO activity (maximum ∼130%) compared with the native XO was observed when the concentration of GdnHCl is not >0.2 M. The activity decreased gradually when the concentration of GdnHCl is >0.2 M, and a complete loss of enzymatic activity was observed when 3.0 M GdnHCl is reached [**Fig. 2(C)**]. The addition of FAD afforded a remarkable protection against the inactivation of XO by GdnHCl under mildly denaturing conditions, in which an enhancement in xanthine oxygen reductase activity (maximum ∼140%) compared with the native XO was observed, but could not protect against the inactivation when 3.0 M GdnHCl is reached [**Fig. 2(C)**]. These results suggest that conformational changes of XO may occur subsequent to flavin loss and is irreversible after FAD has been removed in the presence of a strong denaturing agent. In order to find out which domain is responsible for the activity change of XO, XO activity was further measured using various electron acceptors such as DCPIP which is molybdenum dependent but not FAD dependent. As shown in the inset of **Fig. 2(C)**, the addition of DCPIP also afforded a remarkable protection against the inactivation of XO by GdnHCl under mildly denaturing conditions, but could not protect against the inactivation when 3.0 M GdnHCl is reached. The above results indicate that the activity change of XO induced by GdnHCl (including an enhancement of XO activity by low concentrations of GdnHCl) is dependent on both the FAD domain and the molybdopterin-binding domain.

For studying the reversibility of the GdnHCl-denatured catalase and XO, refolding studies were performed. The two enzymes were incubated with increasing concentrations of GdnHCl for 15 h at 4°C, and then diluted 20 fold (for catalase) and 60 fold (for XO) into phosphate buffer (pH

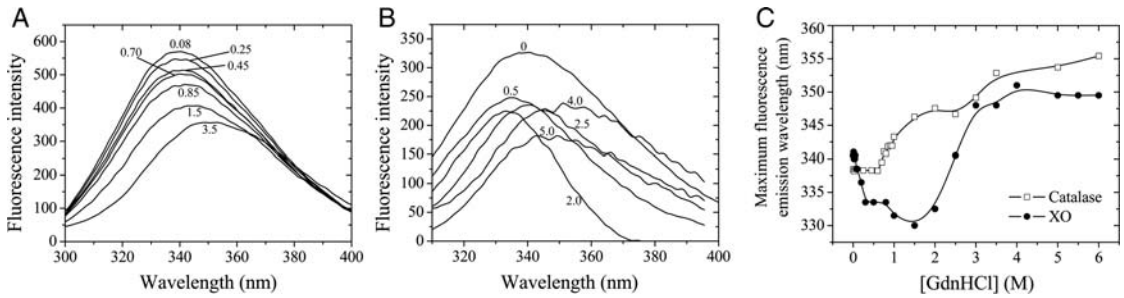

Figure 3 Structural changes of catalase and XO at different concentrations of GdnHCl Structural changes of catalase (A) and XO (B) at different concentrations of GdnHCl monitored by intrinsic fluorescence emission. Denaturant concentration values in M are indicated in the vicinity of the corresponding curve. (C) Effect of GdnHCl on fluorescence maximum emission wavelength of both enzymes. The excitation wavelengths were 280 and 295 nm for catalase and XO respectively, and the emission data were collected between 300 and 400 nm.

7.4) and placed for 4 h at 4°C. The extent of renaturation of both enzymes was judged by the recovery of enzymatic activity. **Figure 2(B,D)** show the refolding yields of GdnHCl-treated catalase and XO samples. As shown in **Fig. 2(B)**, an enhancement in activity (maximum ~110%) compared with the native catalase was observed by dilution of catalase incubated with GdnHCl at concentrations not >0.5 M into the refolding buffer, but the yield of reactivation was zero when the concentration of GdnHCl is >1.8 M. As shown in **Fig. 2(D)**, the activity regained completely and an enhancement in activity (maximum ~130%) compared with the native XO was observed by dilution of XO incubated with GdnHCl at concentrations not >2.0 M into the refolding buffer, but the yield of reactivation was zero when the concentration of GdnHCl is >3.0 M either in the absence or in the presence of FAD. These observations demonstrated that complete refolding to native catalase and XO could be achieved after denaturation of both enzymes with low or intermediate denaturant concentrations, whereas denaturation at high denaturant concentrations was irreversible, resulting in the inability to recover native protein upon refolding. Besides, the loss of activity for XO induced by GdnHCl was associated with flavin released. Once FAD was dissociated from the enzyme induced by GdnHCl, the activity was lost irreversibly.

Two intermediates exist in the conformational changes of catalase and XO

Since the spectral parameters of fluorescence emission spectra such as position, shape, and intensity are dependent on the electronic and dynamic properties of the chromophore environments, steady state fluorescence has been extensively used to obtain the information on the structural and dynamic properties of a protein [18]. **Figure 3(A,C)** summarizes the effects of increasing GdnHCl on the fluorescence spectra of native catalase. As shown in **Fig. 3(A)**, the fluorescence emission peak of catalase was decreasing with the increasing concentration of GdnHCl, and the emission maximum of the protein was red-shifted gradually between 0.65 and 6.0 M GdnHCl. As shown in **Fig. 3(C)**, an obvious plateau region representing the first conformational transition of catalase was observed between 0 and 0.65 M GdnHCl. The second transition was observed between 0.65 and 2.5 M GdnHCl. When the concentration of GdnHCl increased up to 6.0 M, the emission maximum was red-shifted to 356 nm, indicating the third transition. This indicated that the unfolding of catalase induced by GdnHCl was not an all-or-none transition procedure but followed a four-state model.

The modification of microenvironment of aromatic residues of XO due to denaturants has been studied by monitoring the changes in intensity and emission maximum as a function of denaturant concentrations [29]. The contribution of tryptophan and FAD to the total fluorescence of the protein was significant when XO was excited at 295 and 450 nm. **Figure 3(B,C)** shows GdnHCl-induced changes in tryptophan emission wavelength of XO over a wide range of denaturant concentrations. As shown in **Fig. 3(C)**, the tryptophan emission maximum of XO was blue-shifted from 341 nm of the native form to 330 nm of a partially folded intermediate with the concentration of GdnHCl increasing from 0 to 1.5 M, indicating that tryptophan residues were gradually buried in a more hydrophobic environment within such a concentration range of denaturant. When the concentration of GdnHCl is >1.5 M however, the tryptophan emission maximum of XO was red-shifted from 330 nm of a partially folded intermediate to 348 nm of another intermediate at 3.0 M GdnHCl, indicating that tryptophan residues were gradually expose to a more hydrophilic environment under such conditions. Complete unfolding of XO occurred at 4.0 M GdnHCl. The above results indicated that the unfolding of XO induced by GdnHCl also followed a four-state model.

Figure 4(A) shows a phase diagram representing the unfolding of catalase induced by GdnHCl, designed using the 'phase diagram' method of fluorescence. As shown in **Fig. 4(A)**, the conformational transition from the native

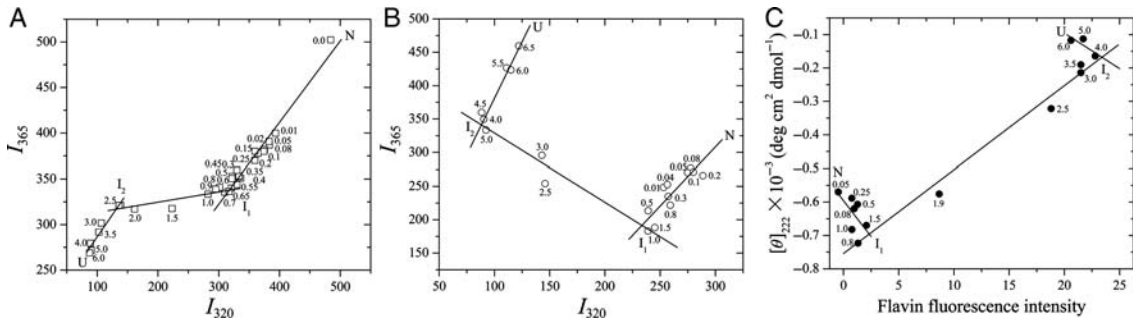

Figure 4 Phase diagrams representing the unfolding of catalase and XO induced by GdnHCl denaturant concentration values in M are indicated in the vicinity of the corresponding symbol. (A) A phase diagram based on intrinsic fluorescence intensity of catalase measured on wavelengths 320 and 365 nm. Each straight line represents an all-or-none transition between two conformers of catalase, denoted as N (the native tetramer), I_1 (partially folded active intermediate), I_2 (partially folded inactivated monomer) and U (the unfolded state). (B) A phase diagram based on the intrinsic fluorescence intensity of XO measured on wavelengths 320 and 365 nm. (C) A 'mixed' phase diagram based on the flavin fluorescence intensity of XO and far-UV CD data ($[\theta]_{222}$). Each straight line represents an all-or-none transition between two conformers of XO, denoted as N (the native state), I_1 (intermediate bound by FAD partially), I_2 (intermediate with FAD completely dissociated) and U (the unfolded state).

tetramer (N) to the first intermediate I_1 of catalase occurred in the concentration range of GdnHCl from 0 to 0.65 M, and the second transition from I_1 to the second intermediate I_2 of catalase took place between 0.65 and 2.5 M GdnHCl. The third transition from I_2 to the completed unfolded state (U) occurred between 2.5 and 6.0 M GdnHCl. The above results once again indicated that the unfolding of catalase followed a four-state model. Similarly, two intermediates existed in the conformational changes of XO induced by GdnHCl. As shown in **Fig. 4(B,C)**, the conformational transition from the native state (N) to the first intermediate I_1 of XO, bound by FAD partially, occurred in the concentration range of GdnHCl from 0 to 1.5 M. The second transition from I_1 to the second intermediate I_2 of XO, with FAD completely dissociated, took place between 1.5 and 3.0 M GdnHCl. The third transition from I_2 to the unfolded state (U) occurred between 3.0 and 6.0 M GdnHCl. These results once again indicated that the unfolding of XO followed a four-state model.

The intensity of FAD fluorescence remarkably increases when a FAD-containing protein is denatured with FAD gradually dissociated [16,17]. **Figure 5(A)** summarizes the effect of GdnHCl on flavin fluorescence intensity of XO. At low concentrations of GdnHCl (0–1.0 M), the flavin fluorescence intensity did not change compared with the native enzyme, indicating that such low concentrations of GdnHCl could not induce FAD to dissociate from XO. An increase in GdnHCl concentration from 1.0 to 3.0 M resulted in a strong increase in FAD fluorescence intensity, indicating that FAD was gradually dissociated from the first intermediate of XO, forming the second intermediate. Further increasing GdnHCl concentration up to 6.0 M showed no further change in flavin fluorescence intensity, indicating that FAD was completely dissociated from both the second intermediate and the unfolded state of XO [**Fig. 5(A)**].

Acrylamide quenches the fluorescence of surface-exposed and partially buried tryptophan residues but not those buried in the hydrophobic core of a protein.

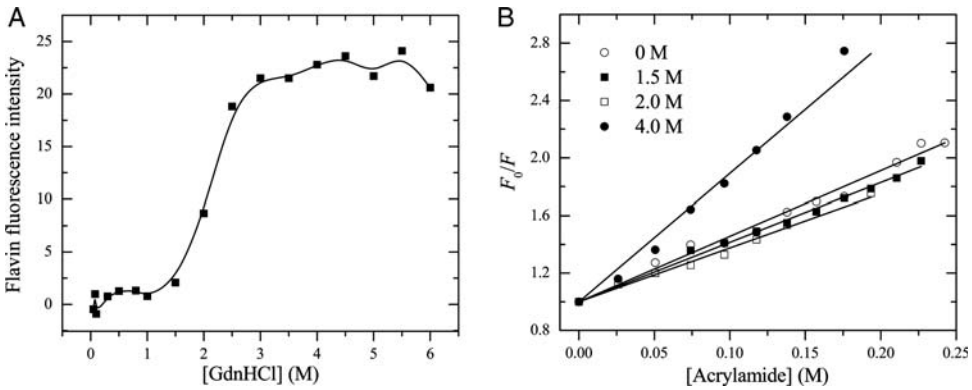

Figure 5 Flavin fluorescence change and acrylamide quenching of tryptophan fluorescence of XO induced by GdnHCl (A) Effect of GdnHCl on flavin fluorescence intensity of XO. The excitation wavelength was 450 nm and the emission data were collected between 500 and 600 nm. (B) Stern–Volmer plots of acrylamide quenching of tryptophan fluorescence of XO in the absence (open circle) and presence of GdnHCl. The concentrations of GdnHCl were 1.5 (solid square), 2.0 (open square), and 4.0 (solid circle) M, respectively. The excitation wavelength was 295 nm and the concentration of XO was 0.17 μM. Experiments were performed at 25°C.

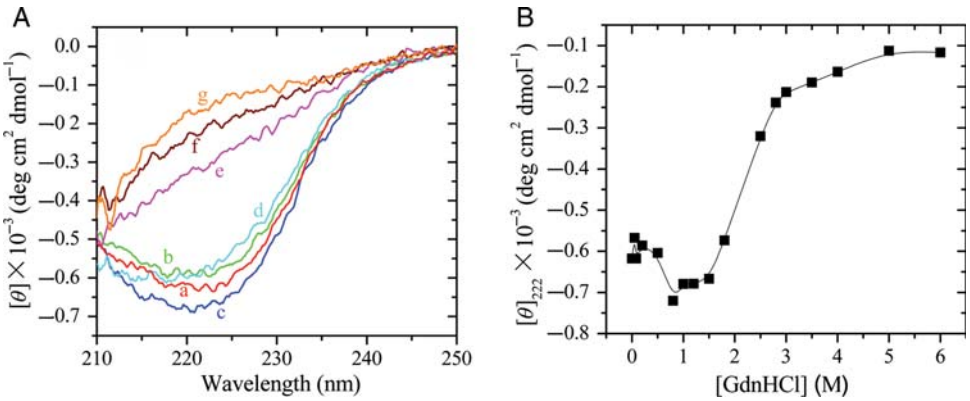

Figure 6 GdnHCl-induced secondary structural changes of XO (A) Far-UV CD spectra of XO. Curves a, b, c, d, e, f, and g represent the spectra of native XO and XO in the presence of 0.2, 1.0, 1.8, 2.5, 3.0, and 4.0 M GdnHCl, respectively. (B) Effect of GdnHCl on the α-helical content of XO, studied by monitoring the CD signal at 222 nm. The concentration of XO was 0.73 μM. Experiments were performed at 25°C.

Therefore, acrylamide quenching has been used to provide insights into conformational changes of proteins by probing the solvent accessibility of fluorescent moieties [15,29–31]. **Figure 5(B)** shows Stern–Volmer plots for the tryptophan fluorescence quenching of XO by acrylamide at different concentrations of GdnHCl. Stern–Volmer quenching constants (K_{SV}) can be obtained from the slope of each linear relationship. As shown in **Fig. 5(B)**, native XO was characterized by a K_{SV} of $4.55 \pm 0.08\ M^{-1}$, indicating five of nine tryptophan residues of native XO, a rigid globular protein, were exposed to a more hydrophilic environment. A small decrease in the solvent accessibility of tryptophan residues was observed at 1.5 and 2.0 M GdnHCl showing only four of nine tryptophan residues of the first intermediate of XO were exposed to a more hydrophilic environment [**Fig. 5(B)**], which is consistent with the data from the intrinsic fluorescence experiments [**Fig. 3(C)**]. The unfolded state of XO, induced by 4.0 M GdnHCl, was characterized by a K_{SV} of $8.98 \pm 0.44\ M^{-1}$, indicating that all of the nine tryptophan residues of XO [28] were exposed to a more hydrophilic environment, in perfect agreement with the data from the intrinsic fluorescence experiments [**Fig. 3(C)**].

The effect of increasing GdnHCl concentration on the secondary structure of XO was investigated by far-UV CD. **Figure 6(A)** shows the Far-UV CD spectra of XO in the presence of GdnHCl at different concentrations, and **Fig. 6(B)** displays GdnHCl concentration dependence of the α-helical content of XO. In the far-UV region, native XO showed a CD spectrum indicating the presence of substantial α-helical conformation [**Fig. 6(A)**]. The relative change in the α-helical content of XO, represented by the relative change in ellipticity of the enzyme at 222 nm, was calculated from the CD spectra. As shown in **Fig. 6(B)**, the absolute value of $[\theta]_{222}$ of XO in the presence of 1.0–1.5 M GdnHCl was larger than that in the absence of GdnHCl, indicating that the α-helical content of the first intermediate of XO was larger than that of native XO. An increase in GdnHCl concentration from 1.5 to 3.0 M resulted in a steep decrease in the α-helical content of XO, indicating that the α-helical content of the second intermediate of XO was much smaller than that of the native XO. The absolute value of $[\theta]_{222}$ of XO in the presence of 4.0–6.0 M GdnHCl was very small, indicating the unfolded state of the protein only contained a very small amount of secondary structures (**Fig. 6**).

All the above results demonstrate that two structurally distinct species exist in the conformational changes of XO induced by GdnHCl. One species populates around 1.5 M GdnHCl characterized as a compacted intermediate bound by FAD partially, whose α-helical conformation is richer than that of the native XO, and the other accumulates around 3.0 GdnHCl characterized as a flexible intermediate with FAD completely dissociated and contains only a small amount of secondary structures.

Discussion

A novel finding of this work is that low concentrations of GdnHCl can activate both catalase and XO to some extent. GdnHCl is an electrolyte with a pK_a of ~11. Thus, at physiological pH, at which our experiments were performed, the GdnHCl molecule will be present in a fully dissociated form as a Gdn^+ cation and Cl^- anion. Protein stabilization/activation by GdnHCl originates from (i) protein stiffening or entropic effect due to the cross-linking action of $GdnH^+$ cations and/or (ii) electrostatic effect due to the interaction of Cl^-, and also possibly of $GdnH^+$, with charged groups of the protein [32–36]. It has been reported that GdnHCl exerts dual effects on the tryptophan synthase $\alpha_2\beta_2$ complex as a cation activator and as a modulator of the active site conformation [34]. An enhancement in the catalase/XO activity (maximum ~115%/130%) compared with the native catalase/XO was

observed in the presence of low concentrations of GdnHCl, but the addition of NaCl up to 1.0 M had no obvious effect on the activities of both catalase and XO (data not shown). These results suggested that low concentrations of GdnHCl activated these two multidomain oxidoreductases predominantly by entropic effect, modulating the active site conformation of both enzymes, and electrostatic interactions did not play an important role in such processes. Interestingly, the influence of GdnHCl on the conformation and activity of XO has been reported by a recent paper [37]. XO activity in the presence of NAD^+ appears to be increased by the treatment of low concentrations of GdnHCl [37], supporting the observation mentioned above. Furthermore, according to the three dimensional structures of XO determined by X-ray crystallography [9] and conformational changes particularly on XO (this work and [37]), we proposed that low concentrations of GdnHCl could induce structural changes of the FAD and molybdopterin domains of XO mainly by entropic effect, resulting in a dramatic change of the FAD-approaching active site loop's conformation and an enhancement of XO activity.

Our data provide evidence that the equilibrium unfolding of catalase and XO in GdnHCl follows a similar pathway. The unfolding of catalase induced by GdnHCl followed a four-state model. With increasing the concentration of GdnHCl from 0 to 0.65, 2.5 and 6.0 M, the conformation of catalase is changed from the native tetramer into a partially folded active dimer (maximum 115%), which is disassembled from the native tetramer and activated by GdnHCl, a partially folded inactivated monomer and the unfolded state, respectively. The unfolding of XO induced by GdnHCl also followed a four-state model. With increasing concentration of GdnHCl from 0 to 1.5, 3.0 and 6.0 M, the conformation of XO is changed from the native state bound by FAD completely into an active, compacted intermediate bound by FAD partially and activated by GdnHCl, an inactive flexible intermediate with FAD completely dissociated and the unfolded state, respectively. The formation of these two intermediates during XO unfolding is possibly attributed to the existence of cofactors such as FAD. The partial dissociation and complete dissociation of FAD from XO could induce remarkable conformational changes in the enzyme. It has been reported that XO activity in the presence of NAD^+ is decreased drastically when 3.0 M GdnHCl is reached, presumably because of extensive protein unfolding induced by high concentrations of GdnHCl [37]. When nuclear magnetic resonance data for several small proteins are combined with hydrodynamic and small-angle X-ray scattering data, the picture emerges that protein chains are relatively compact under mild denaturing conditions, forming intermediates sometimes referred to as molten globules [38–40]. In the present study, we observed such a compacted intermediate for a big protein, XO, under mild denaturing conditions, whose α-helical conformation was even richer than that of the native XO and was bound by FAD partially.

In conclusion, two intermediates including a partially folded active intermediate exist in the conformational changes of both catalase and XO induced by GdnHCl. The addition of FAD affords a remarkable protection against XO inactivation by GdnHCl under mildly denaturing conditions. These findings provide impetus for exploring the influences of cofactors such as FAD on the structure–function relationship of xanthine oxidoreductases.

Funding

This work was supported by the grants from the National Key Basic Research Foundation of China (2006CB910301), and National Natural Science Foundation of China (30770421 and 30970599).

References

1 Zámocký M and Koller F. Understanding the structure and function of catalases: clues from molecular evolution and *in vitro* mutagenesis. Prog Biophys Mol Biol 1999, 72: 19–66.
2 Lardinois OM, Mestdagh MM and Rouxhet PG. Reversible inhibition and irreversible inactivation of catalase in presence of hydrogen peroxide. Biochim Biophys Acta 1996, 1295: 222–238.
3 Prakash K, Prajapati S, Ahmad A, Jain SK and Bhakuni V. Unique oligomeric intermediates of bovine liver catalase. Protein Sci 2002, 11: 46–57.
4 Masters C, Pegg M and Crane D. On the multiplicity of the enzyme catalase in mammalian liver. Mol Cell Biochem 1986, 70: 113–120.
5 Reid TJ, 3rd, Murthy MR, Sicignano A, Tanaka N, Musick WD and Rossmann MG. Structure and heme environment of beef liver catalase at 2.5 Å resolution. Proc Natl Acad Sci USA 1981, 78: 4767–4771.
6 Blanco E, Ruso JM, Prieto G and Sarmiento F. Different thermal unfolding pathways of catalase in the presence of cationic surfactants. J Phys Chem B 2007, 111: 2113–2118.
7 Zhou YL, Liao JM, Chen J and Liang Y. Macromolecular crowding enhances the binding of superoxide dismutase to xanthine oxidase: implications for protein-protein interactions in intracellular environments. Int J Biochem Cell Biol 2006, 38: 1986–1994.
8 Harris CM, Sanders SA and Massey V. Role of the flavin midpoint potential and NAD binding in determining NAD versus oxygen reactivity of xanthine oxidoreductase. J Biol Chem 1999, 274: 4561–4569.
9 Enroth C, Eger BT, Okamoto K, Nishino T and Pai EF. Crystal structures of bovine milk xanthine dehydrogenase and xanthine oxidase: structure-based mechanism of conversion. Proc Natl Acad Sci USA 2000, 97: 10723–10728.
10 Harris CM and Massey V. The oxidative half-reaction of xanthine dehydrogenase with NAD; reaction kinetics and steady-state mechanism. J Biol Chem 1997, 272: 28335–28341.
11 Hille R and Nishino T. Flavoprotein structure and mechanism. 4. Xanthine oxidase and xanthine dehydrogenase. FASEB J 1995, 9: 995–1003.
12 Ichida K, Ayama Y, Noda K, Minoshima S, Hosoya T, Sakai O and Shimizu N, *et al*. Cloning of the cDNA encoding human xanthine dehydrogenase (oxidase): structural analysis of the protein and chromosomal location of the gene. Gene 1993, 133: 279–284.

13 McManaman JL and Bain DL. Structural and conformational analysis of the oxidase to dehydrogenase conversion of xanthine oxidoreductase. J Biol Chem 2002, 277: 21261–21268.
14 Liang Y, Du F, Sanglier S, Zhou BR, Xia Y, Dorsselaer AV and Maechling C, *et al*. Unfolding of rabbit muscle creatine kinase induced by acid. A study using electrospray ionization mass spectrometry, isothermal titration calorimetry, and fluorescence spectroscopy. J Biol Chem 2003, 278: 30098–30105.
15 Yang F, Jr, Zhang M, Zhou BR, Chen J and Liang Y. Structural changes of α-lactalbumin induced by low pH and oleic acid. Biochim Biophys Acta 2006, 1764: 1389–1396.
16 van den Berg PAW, Feenstra KA, Mark AE, Berendsen HJC and Visser AJWG. Dynamic conformations of flavin adenine dinucleotide: simulated molecular dynamics of the flavin cofactor related to the time-resolved fluorescence characteristics. J Phys Chem B 2002, 106: 8858–8869.
17 Maskevich AA, Artsukevich IM and Stepuro VI. Fluorescence properties of the alcohol oxidase prostethic group and their relationship to the functional state of proteins. J Mol Struct 1997, 409: 261–264.
18 Prajapati S, Bhakuni V, Bab KR and Jain SK. Alkaline unfolding and salt-induced folding of bovine liver catalase at high pH. Eur J Biochem 1998, 255: 178–184.
19 Góth L. A simple method for determination of serum catalase activity and revision of reference range. Clin Chim Acta 1991, 196: 143–152.
20 Özer N, Müftüoglu M, Ataman D, Ercan A and Ögüs IH. Simple, high-yield purification of xanthine oxidase from bovine milk. J Biochem Biophys Methods 1999, 39: 153–159.
21 Massey V, Brumby PE and Komai H. Studies on milk xanthine oxidase. Some spectral and kinetic properties. J Biol Chem 1969, 244: 1682–1691.
22 Linder N, Martelin E, Lapatto R and Raivio KO. Posttranslational inactivation of human xanthine oxidoreductase by oxygen under standard cell culture conditions. Am J Physiol Cell Physiol 2003, 285: C48–C55.
23 Bushmarina NA, Kuznetsova IM, Biktashev AG, Turoverov KK and Uversky VN. Partially folded conformations in the folding pathway of bovine carbonic anhydrase II: a fluorescence spectroscopic analysis. Chem Bio Chem 2001, 2: 813–821.
24 Zhou BR, Liang Y, Du F, Zhou Z and Chen J. Mixed macromolecular crowding accelerates the oxidative refolding of reduced, denatured lysozyme: implications for protein folding in intracellular environments. J Biol Chem 2004, 279: 55109–55116.
25 Kuznetsova IM, Turoverov KK and Uversky VN. Use of the phase diagram method to analyze the protein unfolding-refolding reactions: fishing out the 'invisible' intermediates. J Proteome Res 2004, 3: 485–494.
26 Yang F, Jr, Zhang M, Zhou BR, Chen J and Liang Y. Oleic acid inhibits amyloid formation of the intermediate of α-lactalbumin at moderately acidic pH. J Mol Biol 2006, 362: 821–834.
27 Ludwig HC, Pardo FN, Asenjo JL, Maureira MA, Yañez AJ and Slebe JC. Unraveling multistate unfolding of pig kidney fructose-1,6-bisphosphatase using single tryptophan mutants. FEBS J 2007, 274: 5337–5349.
28 Jenkins DC, Sylvester ID and Pinheiro TJ. The elusive intermediate on the folding pathway of the prion protein. FEBS J 2008, 275: 1323–1335.
29 Sau AK and Mitra S. Steady state and picosecond time-resolved fluorescence studies on native, desulpho and deflavo xanthine oxidase. Biochim Biophys Acta 2000, 1481: 273–282.
30 Kuznetsova IM, Stepanenko OV, Turoverov KK, Zhu L, Zhou JM, Fink AL and Uversky VN. Unraveling multistate unfolding of rabbit muscle creatine kinase. Biochim Biophys Acta 2002, 1596: 138–155.
31 Rust E, Martin DL and Chen CH. Cofactor and tryptophan accessibility and unfolding of brain glutamate decarboxylase. Arch Biochem Biophys 2001, 392: 333–340.
32 Bhuyan AK. Protein stabilization by urea and guanidine hydrochloride. Biochemistry 2002, 41: 13386–13394.
33 Karmodiya K and Surolia N. A unique and differential effect of denaturants on cofactor mediated activation of *Plasmodium falciparum* β-ketoacyl-ACP reductase. Proteins 2008, 70: 528–538.
34 Fan YX, McPhie P and Miles EW. Guanidine hydrochloride exerts dual effects on the tryptophan synthase $\alpha_2\beta_2$ complex as a cation activator and as a modulator of the active site conformation. Biochemistry 1999, 38: 7881–7890.
35 Zhang HJ, Sheng XR, Pan XM and Zhou JM. Activation of adenylate kinase by denaturants is due to the increasing conformational flexibility at its active sites. Biochem Biophys Res Commun 1997, 238: 382–386.
36 Fan YX, Ju M, Zhou JM and Tsou CL. Activation of chicken liver dihydrofolate reductase by urea and guanidine hydrochloride is accompanied by conformational change at the active site. Biochem J 1996, 315: 97–102.
37 Tsujii A and Nishino T. Mechanism of transition from xanthine dehydrogenase to xanthine oxidase: effect of guanidine-HCl or urea on the activity. Nucleos Nucleot Nucleic Acids 2008, 27: 881–887.
38 Shortle D and Ackerman MS. Persistence of native-like topology in a denatured protein in 8 M urea. Science 2001, 293: 487–489.
39 Kuwajima K. The molten globule state as a clue for understanding the folding and cooperativity of globular-protein structure. Proteins 1989, 6: 87–103.
40 Vassilenko KS and Uversky VN. Native-like secondary structure of molten globules. Biochim Biophys Acta 2002, 1594: 168–177.